Basrah Journal for Engineering Sciences, Vol. 22, No. 1, (2022), 1-8

BJES Basrah Journal for Engineering Sciences

Original Article

Journal homepage: www.bjes.edu.iq
ISSN (Online): 23118385, ISSN (Print): 18146120

OPEN ACCESS

2-D Actuator based Shape Memory Alloy using PID controller

Hassan Falah Abdulkadhim [1, *], Abdulkareem F. Hassan [2], Ali H. Abdulaali [3]

[1, 2, 3] *Department of Mechanical Engineering, College of Engineering, University of Basrah, Basrah, Iraq*
E-mail addresses: hassan.f1991@gmail.com , abdulkareem.flaih@uobasrah.edu.iq , ali.abdulali@uobasrah.edu.iq
Received: 3 September 2021; Accepted: 23 September 2021; Published: 24 April 2022

Abstract

Over the past years, researchers have been focusing on development the robotics and actuation due to increase demand for these applications like industrial engineering, oil industry, healthcare, aerospace … etc. This work involves the design, construction and control of the Shape Memory Alloy (SMA) actuator. The industrial actuator has many characteristics able to be measured, which have an impact on the efficiency and effectiveness of the actuator while the execution of its tasks. The most important measurable characteristics are repeatability and accuracy. The current system typically is using Nitinol (Nickle Titanium Naval Ordinance Lab), which is one of the Shape Memory Alloy that contract when applying specific heat on it, and it can be used as an actuator. This work presents SMA in the shape of a spring to operate and control the accurate position of the 2-D system which containing four SMA springs, two SMA springs for the *x*-axis and two SMA springs for the *y*-axis. The theoretical design and calculations for SMA springs have been presented to collect information about the SMA springs. In a practical manner, the SMA spring characteristic like force and displacement were collected by a test bed that was designed and constructs before making the final rig.

The setting shape of the SMA spring was presented and done as per the theoretical calculations. In the rig, each axis works as a two-direction actuator, the actuator is not prone to precise position points due to hysteresis and temperature variation.

The SMA spring exhibited hysteresis and imprecise pointing, for that employing PID (Proportional Integral Derivative) with tracking mode controller to compensate the hysteresis. PID control system is played a decisive role with tracking mode model that achieves the aim behind the construction of the experimental rig. Good results have been obtained presented in three cases of drawing different shapes.

Keywords: 2-D SMA actuator, PID controller, SMA spring, SMA spring cooling/heating response.

https://dx.doi.org/10.33971/bjes.22.1.1

1. Introduction

In this technological age, the use of robotics and actuation as a key component in diverse technology and science have attracted more interested. The development and technology progress in scientific fields furthermore the industrial competition between designers as well as manufactures, is a result of human requirements for new technologies to manage this process. The actuator or robotics is currently a major source for doing a task on behalf of human and it will replace humans and humans' activities. Actuation is a branch of engineering and science that consists of mechanical engineering, electronics engineering and computer science and so on. The actuator deals with design, aspect construction, sensor feedback and information processing. The new technology trying to be easier to make the cover of the massive progressing in development. The actuator being more complicated in design and manufacturing due to complications in an electronic system. Shape memory alloy (SMA) one of the smart materials that can overcome the electronic complication, SMA has the ability to recover its shape while rising temperature, some authors like Andrianesis et al. [1] present that. The unique features of SMA make them one of the attractive materials which suitable for engineering applications such diverse areas as aerospace, actuation and biomedical engineering. Brinson [2] presented one-dimensional constitutive behavior of shape memory alloys: thermomechanical derivation with non-constant material functions and redefined martensite internal variable. To derive constitutive comprehensive law for SMAs, the internal variable approach is used without the assumption of constant material functions from the first principle. This constitutive law can be justified; it is a form that is proper for calculation and engineering application. More accurately, constitutive law was derived to capture the internal variable for separation martensite fraction into stress-induced and temperature-induced parts. Pseudoplastic and shape memory effect is presented at all temperatures. To take over the thermomechanical behavior for SMAs through internal phase transformations with temperature and stress, several numerical examples are presented that explain the ability of constitutive law. Brinson's model satisfies all statuses only when the stress increases or only the temperature decreases. Liang et al. [3] presented one-dimensional thermomechanical constitutive relations for shape memory materials. The thermomechanical constitutive model has investigated the main characteristics of the material that involved the internal phase transformation of SMAs. Many SMAs characteristics have been emphasized and presented which include energy dissipation, SME and strain-stress-temperature relation of pseudoplasticity. Proposed the equation to fit the relations between temperature and martensite fraction in order to predict shape memory behavior and stress-strain relation. Provided the theoretical guide to

structure and design SMAs due to more focusing on SME behavior. Chung et al. [4] studied the implementation strategy for the dual transformation region in the Brinson SMA constitutive model. The transformation kinetics formulation is a factor that implied the constitutive model of SMAs, therefore thus it is fundamental for predicting the material behavior of SMAs. The limitation of Brinson's model was emphasized and presented which consists of weakness prediction in case of the temperature decreases at low temperature. Modification of the transformation kinetics in the dual transformation region of martensite is also presented based on the Brinson model. Through this modification, the proposed formulation can well be suited to describe the martensite fractions behavior in the dual transformation region. Nunes et al. [5] presented the influence of the SMA constitutive model on the response of the structures. The effect of earthquakes may impose significant damages or displacements in structures. A design and analysis of this model were performed a using two-degree-of-freedom model, which consists of two reinforced concrete frames with variable nature vibration periods connected by SMA bars. The result showing that the relative displacements are more sensitive to the SMA model and less sensitive to absolute displacements, based on numerical analysis that conducted by MATLAB to evaluate the influence of many kinetic laws of the response of the structure. Lange et al. [6] studied SMAs as linear drives in robot hand actuation. Test the applicability of shape memory alloy and employ it as an actuator for robotic hands. Arrange the parallel wire of SMA along the forearm is implemented in the robotic hand after consideration of different designs. Joule heating approach is used to activation of SMA wire. Open and closed loop control is used as a control system and an adaptive PID controller shows good results for the motion at the full range. Gédouin et al. [7] described the model that deals with industrial applications, most of control strategies applied to SMA actuators are not suitable sometimes for industrial applications. In this paper, researchers deal with a new application of the framework of model-free control (MFC) of an actuator based SMA-spring. Fast derivative estimation of noisy signals is the main control strategy that relies on this work, the robustness and simplicity are the main advantages. Experimental results on an actuator-based SMA-spring show good robustness and good tracking performance towards load variation, thermal disturbance, and final displacement variation for the controllers. Roshan et al. [8] presented a PID controller model to the control SMA spring actuator. Force variation and characterization were conducted with respect to uncontrolled temperature for analysis. Lag can occur between temperature and force measurements due to the difference between temperature and force sensor's response time. The controlled technique was moreover implemented by developing a PID-based closed-loop controller with a GUI which supports sensor calibration and parameter control. Implements and develop force feedback controlling method for force-sensitive applications technique by using same PID controller to maintain the force by varying SMA temperature accordingly.

2. Modelling of 2-D SMA actuator

Exploring SMA properties is helping us to choose suitable SMA type, size and shape for actuation application.

2.1. Shape memory effect of SMA

The shape memory effect (SME) is the main property of SMA: when there is no applied load, no deformation occurs. However, SMA is deformed easily at a low temperature by externally applied forces. The deformed SMA can be restored to the original shape by applied specific heat. These two phases are called as Martensite and Austenite, respectively. From these observations, it can be known that the shape of SMA depends on the temperature and external stress. Fig. 1 shown the effect of phase transformation on NiTi which was investigated by some researchers [9].

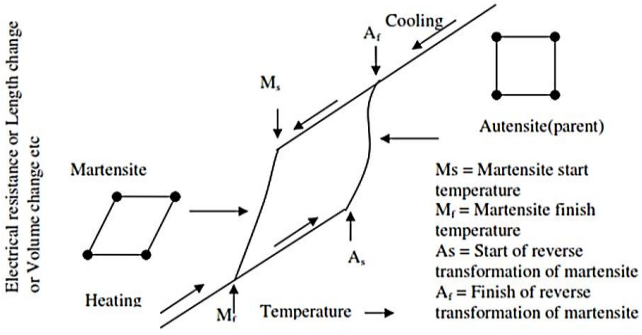

Fig. 1 Effect of phase transformation.

Certainly, the relationship between strain and temperature exhibits a hysteresis phenomenon, this is one difficult to use as a linear actuator.

2.2. Cooling and Heating of SMA

By joule heating law, the passage of the electrical current leading to heat up the SMA material, this is an effective and most popular method to control the temperature of SMA material due to control the amount of power supplied to SMA material. However, a large current is required for heating the SMA wire because the resistance of an SMA wire is small. More current is required for heating if the ambient temperature is low. Therefore, the selection of a suitable power supply is preferred for control under the various environments.

The cooling time has great implications for the response of the system. Employing the effective cooling method will increase the bandwidth of an SMA actuator. There are four popular cooling methods: forced convection cooling (with fan), ice cooling, cooling with running water and cooling with heat sink or Peltier element investigated by Nemat-Nasser et al. [10]. They explored the cooling curve for various cooling methods for NiTi wire, the curve showing that water cooling and heat sink can have a quicker response than air cooling with 1 m/s. The water cooling and heat sink required complex hardware and special design for installation.

2.3. SMA transition temperature

The transition temperature of SMA is playing a major role through effecting by the working environments themselves and the limitation of the application. In the current design, the transition temperature for four springs is 80 °C. Various techniques can be used to direct measuring of the transition temperature such as electrical resistivity measurement as a function of temperature, dilatometry, differential scanning calorimetry (DSC) as shown in Fig. 2, and can be indirectly

determined from a series of constant stress thermal cycling experiments, explored by Ye et al. [11].

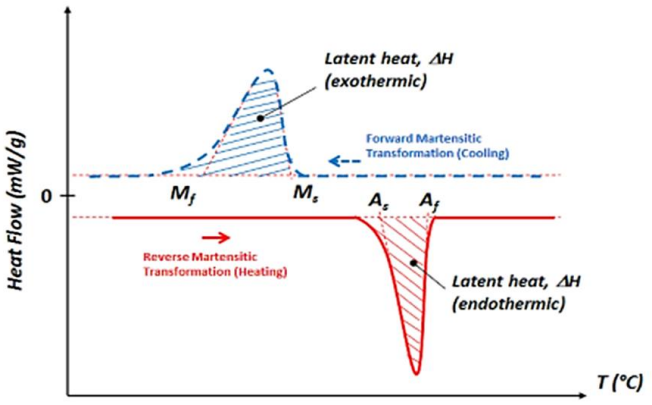

Fig. 2 A typical DSC thermograph of SMA.

SMA mechanical and physical properties varying between martensite and austenite phases, such as electrical resistivity, thermal conductivity, Young's modulus and thermal expansion coefficient. The martensite structure is more malleable and softer; i.e., by application of an external force can be readily deformed, whereas the austenite structure has a much higher Young's modulus and it is relatively hard as shown in Table 1 which proposed by Mihálcz et al. [12].

Table 1. listed the commercial and physical properties of NiTi SMA [12].

Property	Symbol	Units	Value	
			Martensite	Austenite
Corrosion Resistance	-	-	Similar to 300 series SS or Ti-alloy	
Density	ρ_D	kg/m^3	6450 ~ 6500	
Electrical Resistivity (approx.)	ρ_R	μΩ.cm	76 ~ 80	82 ~ 100
Specific Heat Capacity	C	J/kg.K	836.8	836.8
Thermal Conductivity	k	W/m.K	8.6 ~ 10	18
Thermal Expansion Coefficient	α	m/m.k^{-1}	6.6 × 10^{-6}	11.0 × 10^{-6}
Ultimate Tensile Strength	σ_{UTS}	MPa	895 (Fully annealed) / 1900 (Hardened)	
Youngs Modulus (approx.)	E	GPa	28 ~ 41	75 ~ 83
Yield Strength	σ_Y	MPa	70 ~ 140	195 ~ 690
Poisson's Ratio	ν	-	0.33	
Magnetic Susceptibility	χ	μemu.g	2.5	3.8

2.4. Problem statement

In order to develop a 2-D SMA actuator using shape memory alloy. An SMA based-linear actuator which would involve design, construction, and testing will be demonstrated at the test bed. The results were obtained precisely pointing to one degree of freedom accuracy along with one axis to move in two directions. The design of the system was done keeping the following factors in mind:

2.4.1. Precision requirements

SMA's used for actuation application depend on many factors like strain levels, stress levels, type of application and surrounding temperature which restrain their precision in exact amounts of actuation requirements.

2.4.2. SMA temperature control

SMA's are essentially resistors that change phase when a specific value of heat is applied, thus of transformation temperature is reached. There are two ways to heat up SMA's:

a. External heating source
b. Joule heating (providing current)

Temperature control by direct heating is difficult. Thus, their use for passively actuated systems is limited, and that takes into account their transition temperatures. However, a calculated value of power required to heat up wire based on factors like diameter of the wire, length of wire and transition temperature can be used for better actuation results.

In the current design, joule heating has been used and the transition temperature of the SMA wires is 80 °C.

2.4.3. Hysteresis

Fig. 3 shows a typical stress-free temperature-induced martensitic transformation and inverse transformation as well as under a temperature excitation cycle.

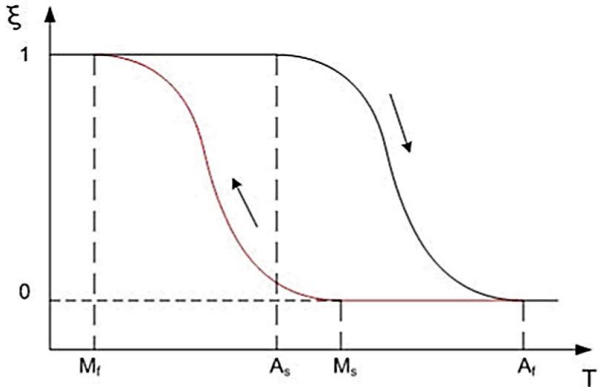

Fig. 3 hysteresis Loop for Shape Memory effect shown by SMA.

From Fig. 3, the transition temperature is characterized by four temperatures which making the transformation loop: Martensite start temperature (Ms), Martensite finish temperature (Mf), Austenite starts temperature (As) and Austenite finish temperature (Af). These critical temperatures are necessary to pinpoint the beginning and the end of the inverse transformation and the forward (Martensite). It is noticeable that the deformation-temperature cycle is hysteretic due to internal phase friction.

2.4.4. Strain rates control

The ratio of force to strain in the SMA wire is limited. SMA properties are adversely affected by straining and the number of cycles they can afford reduces drastically. To operate SMA for millions of cycles, the maximum strain should not exceed 3-4 %.

2.5. SMA spring design specification

In most products, the SMAs are used in coil spring form in order to generate high recovery force, large stroke and function as sensors as well actuators. In the current application, used it as a spring to produce a large stroke with a small force to overcome the friction in the rig axes. Fig. 4 shows the comparison between the coil and straight wire of 30 mm free length, when the given strain is 1.0 % the stroke of the wire is 0.3 mm while the coil spring expands 90.3 mm, which was proposed by Ishii [13].

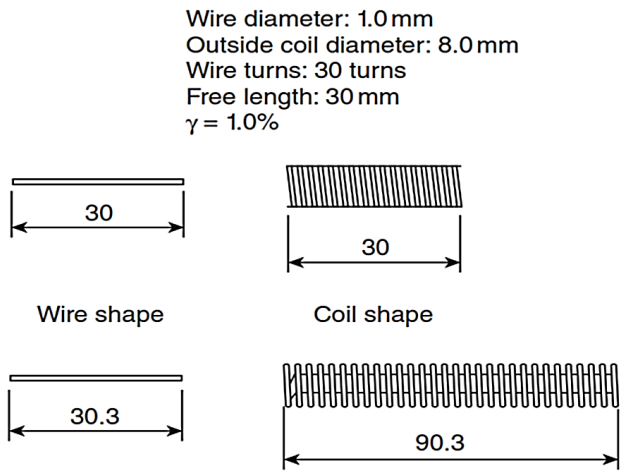

Fig. 4 SMAs comparison stroke between coil shape and wire shape [13].

2.5.1. Difference from usual springs

Conventional springs are designed to work into the elastic region wherever Hooke's law is obeyed. Since the spring constant and shear modulus do not change in the elastic region, it makes the spring design easier. Furthermore, spring constant and shear modulus change with strain, the relation between the load and deflection is not linear for the SMA spring. Moreover, the SMA spring characteristics change greatly with small changes in the composition of the alloy, operating conditions such as strain and temperature, and SMA treatment condition.

2.5.2. SMA shear modulus

The SMA spring shear modulus shows a drastic change when the spring is heated above the martensitic transformation temperature or cooled below it since the shear modulus of the parent phase (high-temperature phase) is ultimately higher than that of the martensite phase (low-temperature phase). For instance, the shear modulus of the martensite phase (low-temperature phase) is about 8000 MPa while that of the parent phase (high-temperature phase) exceeds 20000 MPa in NiTi alloys.

2.5.3. Design of SMA helical spring

The characteristic parameters for the design of SMA springs are summarized in equations below, and Fig. 5 explains the parameters used in the equations.

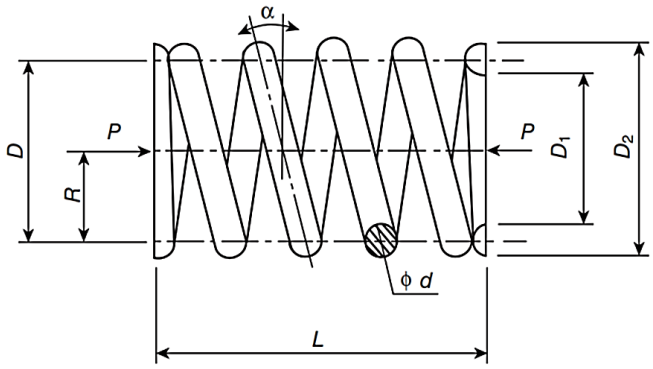

Fig. 5 characteristic parameters of design of an SMA spring [13].

$$\delta = \frac{8\,P\,D^3\,n}{G\,d^4} \tag{1}$$

$$\gamma = \frac{\delta\,d}{\pi\,n\,D^2} \tag{2}$$

$$\tau = \frac{8\,P\,D}{\pi\,d^3} \tag{3}$$

$$G = \frac{\tau}{\gamma} \tag{4}$$

$$C = \frac{D}{d} \tag{5}$$

$$H_s = d\,[(n+2)+1] \tag{6}$$

$$L = 1.25\,\delta_L + H_s \tag{7}$$

2.5.4. Design of SMA spring

In the design condition, many factors were assumed based on the experimental results gathered from the test bed.

The load at high temperature (P = 3 N), chosen this value as per experimental results, this value is suitable to overcome the friction between shafts, linear bearings and moving parts.

The deflection at high-temperature δ_H = 130 mm, deflection per stroke δ_t = 40 mm and deflection at low-temperature $\delta_L = \delta_H + \delta_t$ = 170 mm, chosen these values as per requirements to make the rig moving 110 mm for each axis on working piece.

As mentioned, the shear modulus depends on many factors. SMA wire alloy composition used in the current rig is 57.6 % Nickel and 41.1 % Titanium, lab test show by spectrum device.

From reference [12] the alloy containing 55.3 % Nickel and 43.5 % Titanium, for approximation shear modulus, same shear modulus has been taken.

The shear modulus: G_H = 20000 MPa at the high temperature.

The shear modulus: G_L = 8000 MPa at the low temperature.

2.5.5. SMA spring design calculations

1. Assume mean coil diameter D = 15 mm and wire diameter d = 1 mm. From equation (5), C = 15.
2. The number of coils n is obtained from equation (1) n = 33. If we assume one turn at both ends, the total coils N = 35.
3. Shear strain γ_L at the low temperature is calculated from equation (2), γ_L = 0.0073.
4. Load P_L at the low temperature is obtained from equation (1), P_L = 1.526 N.
5. The solid length H_s of the spring obtained from equation (6), H_s = 36 mm.
6. The free length L of the spring calculated from equation (7) L = 248.5 mm.

3. Experimental setup

The experimental setup is including all the steps needed to make the whole system components interact and communicates together in the right order to make a 2-D SMA actuator actuated by 1 mm and 1.25 mm SMA spring. The hardware control system done by Arduino Mega 2560 and H-bridge. The SMA spring used 1.25 mm in the x-axis because

the friction in the *x*-axis is greater than *y*-axis, 1 mm used in the *y*-axis, also because 1.25 mm and 1 mm were available in the stock. Several controlled parameters of the experimental setup, including the dimension of the actuator and the maximum voltage allowed, were set to allow for repeatability, ensuring that the NiTi spring was deformed reversibly. With the voltage setup, it was verified to keeping the maximum strain below 4 % to prevent structural damage and extend the service life of the NiTi spring. To ensure the correctness of the displacement position of the 2-D actuator, the system was calibrated using a PID controller to capture the right position. The design procedure of the 2-D SMA actuator will illustrate below. The experimental rig design is illustrated in Fig. 6.

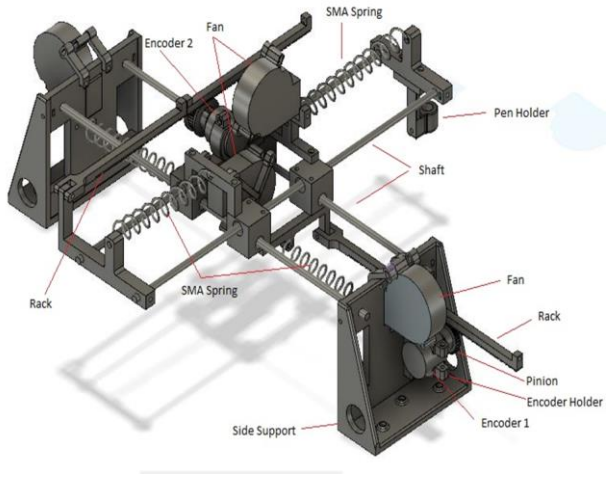

Fig. 6 Main design parts of experimental work.

3.1. Fusion 360 design

It is Autodesk drawing design program; our rig was designed in fusion 360 including overall rig parts as mentioned in Fig. 6. The Fusion 360 environment was easy to draw the rig design parts and to export that to a 3-D printer to print most of the design parts at specific shapes and resolutions.

3.2. Power electronics

For the SMA actuation application, the electrical energy is considered as input to the NiTi spring, in which the alloy is heated by means of the Joule effect through electrical current flow in the SMA spring wire. In the current design, the SMA spring is driven by a PWM modulated controller so that more robust to external disturbance, furthermore, the PWM modulated controller has lower energy consumption than in case-controlled by a continuous signal, while maintaining the same accuracy level, presented by Peciña [14]. The electromechanical transduction by meant of the Joule effect was considered as an activation method for NiTi spring. For theses consideration, four H-Bridge (IBT-2) were used, one for each SMA spring, as a voltage regulator which driven by PWM from Arduino Mega 2560. The H-Bridge insulated the Arduino Mega 2560 and computer from a high current to avoid damage to this equipment.

3.2.1. Measuring voltage

The Arduino Mega 2560 supplies digital output voltage which depends on PWM as well the duty cycle which starts from zero for zero V to 255 for 5 V to control the H-Bridge from zero V to 12 V with a maximum current of 43 A. Based on these considerations, the supply voltage to the SMA spring will be digital not analog voltage, which depends on the duty cycle. The Arduino Mega 2560 board measure only analog voltage, thus a digital to analog converter (DAC) is required for this purpose. The design of the DAC is shown in Fig. 7.

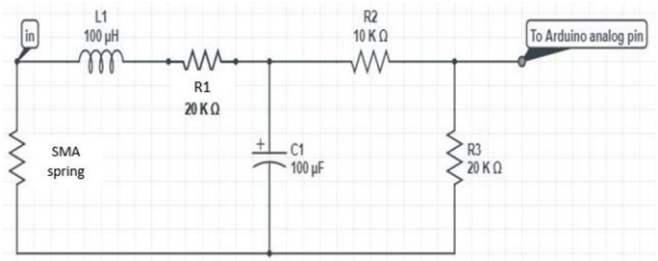

Fig. 7 Digital to Analog converter.

3.2.2. Electronic components

The electronic connection commenced from the computer to the Arduino Mega 2560 then to H-Bridge, as well the two rotary encoders have been connected to Arduino Mega 2560, it was done by wiring the equipment together to get complete electrical circuit. The electronic circuit components are shown in Fig. 8. The main advantage of the H-Bridge is controlling the voltage so that drive required current in the SMA spring.

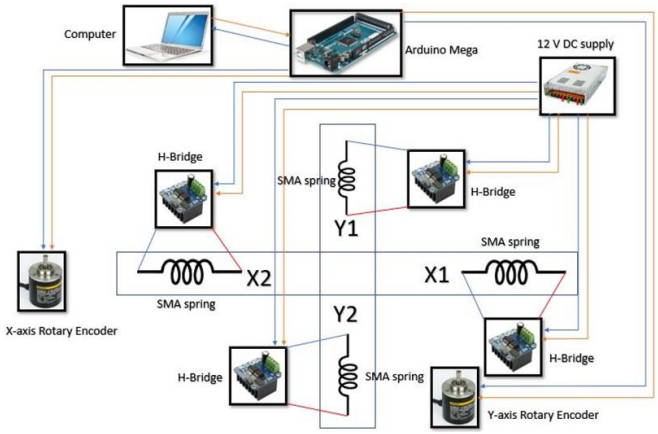

Fig. 8 Rig electronic circuit components.

3.2.3. Bandwidth Determination Experiment

SMA springs were driven via an electrical current being passed through it at room temperature. The current, supplied from a 5 V PWM signal provided by a microcontroller, heats the SMA spring and causes it to contract. This current was applied over a spectrum of frequencies started from 0 to 255 PWM to determine the system bandwidth. To determine at which PWM the SMA spring commences to contract is quite easy, by increasing PWM gradually starting from 0, take into account the wiring resistance as well connection wire length which depend on SMA spring location in the rig. The measured position by the rotary encoder was the system gain to get the required position.

4. PID controller of SMA actuator

The controller design is to minimize the hysteresis of the system and reach out the accurate position required by employing the PID with tracking mode technique approach to do that.

The PID controller that has been presented in the current work will illustrate below.

4.1. PID controller architecture

Recently, the PID controller is one of the popular methods which used for complicated systems. Several auto tunning techniques and robust have been proposed in order to improve PID controller performance, Fig. 9 shown the basic scheme of PID controller. In this study, the PID controller playing a major role in the control of the two axes of the SMA actuator by fed the system required value of PWM which heating up the SMA spring. The presented controller is easy to implement but the main drawback of the controller is how to set the PID parameters.

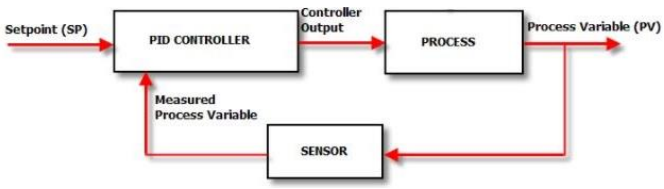

Fig. 9 Simple scheme of PID controller.

4.2. PID tuning

In general, tunning methods can be applied to the PID controller to improve the performance of controller. There are a lot of tunning methods that can be used, since in current controller using a hardware implementation for MatLab/Simulink that is compatible with the Arduino board, and the system operation in Real-Time Workshop (RTW). The tunning methods are not working with RTW because of the time limit of tuning and auto tunning option in the PID controller block. The PID controller has the following values: K_p = 1.6, K_i = 0.06, and K_d = 0.02. These values are not optimized or auto-tuned and were obtained using a trial-and-error basis, which takes a lot of time but is useful in the case of implement the controller on the Arduino board. Limit the PID output between 50 and -50 according to bandwidth operating range. Fig. 10 shows the PID controller set parameters.

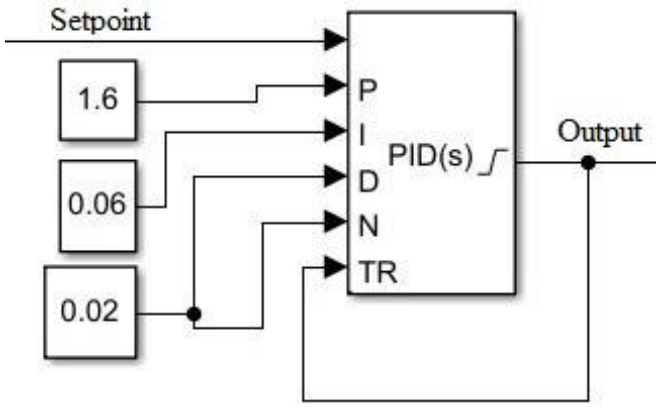

Fig. 10 Set parameters of PID controller.

4.3. position control

For proof-of-concept purposes of the controller is proposed actuator using the PID controller, even though it does not give a better transient response on account of the hysteresis and non-linear behavior of SMA spring. Fig. 11 illustrates a brief diagram of the PID controller scheme to operate two SMA springs. The range of PID output is between -50 to 50 so the mathematical operation adds to the output of PID to switch the value of PID between the two SMA springs their output is switched according to the value of the input position reference. The PID output values from 0 to 50 that activate the first SMA spring and from 0 to -50 that is activated second SMA spring at one axis. The output values of PID represent the output PWM from Arduino to H-Bridge which is determined in the bandwidth determination in the previous section. Additionally, a Simulink saturation block is added to the output of the PID to ensure the PWM remains between a maximum of 50 and a minimum -50.

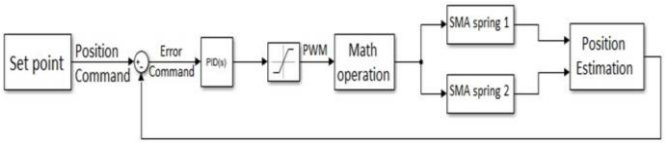

Fig. 11 Brief of PID controller scheme.

5. Results

The verification of the rig drawing has been done by connecting the pencil to the pen holder which is already attached at the end of the *y*-axis of the rig. The experimental rig verification is illustrated below, to present the accuracy of the rig by draw a required square shape (100 mm × 100 mm), the resulting shape which measure by vernier calliper (102.13 mm × 101.23 mm) as shown in Fig. 12.

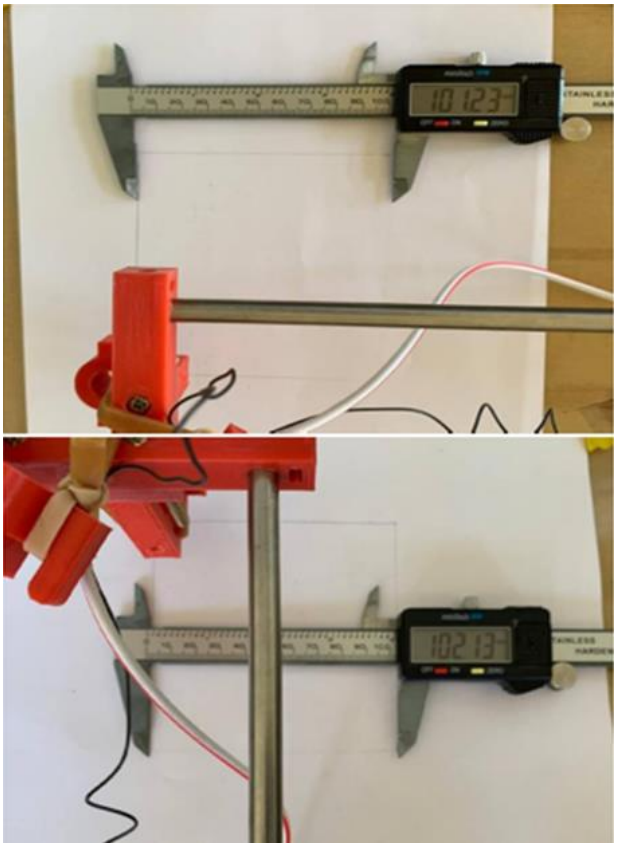

Fig. 12 Square drawing measured by vernier calliper.

5.1. PID tracking for counter displacement

The PID is tracking the set point which out from the displacement counter to achieve good accuracy, so the results of this experiment are plotted in Fig. 13 which explains the actual displacement and set point with time for *x* and *y* axes. The results were good due to good tracking achieved by PID to compensate the error in displacement.

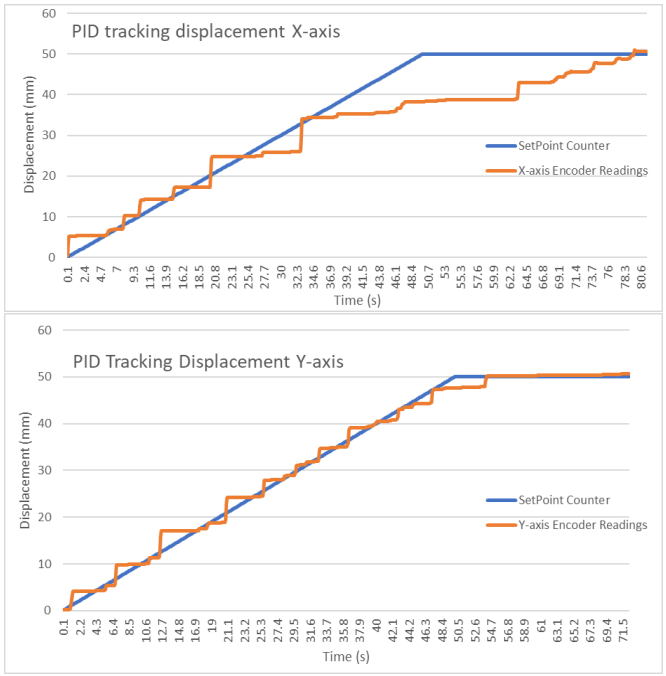

Fig. 13 PID tracking displacement of square drawing.

5.2. Error comparison

Error comparison of drawing one is shown in Fig. 14. The error deviation on the *x*-axis is 1.23 mm and on the *y*-axis is 2.13 mm.

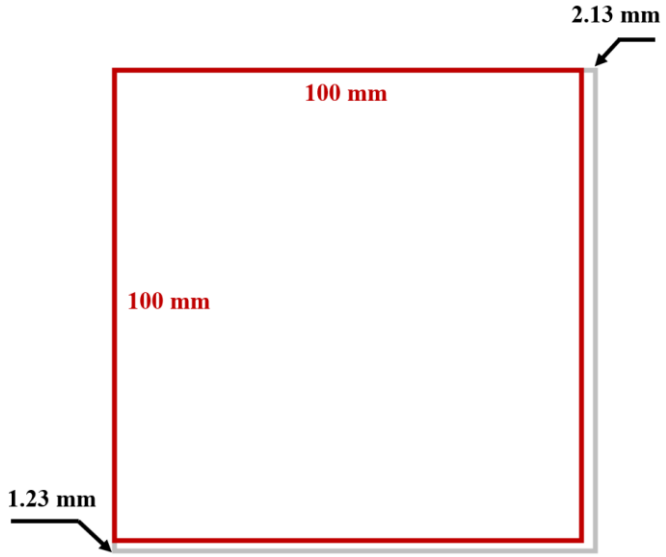

Fig. 14 Case one error comparison.

5.3. RMSE calculation

The RMSE is taken for *x* and *y* axes for displacement tracking to compare between required shape and actual shape as shown in Table 2.

Equation (8) is used to calculate the RMSE value for the *x* and *y* axes.

$$RMSE = \sqrt{\frac{\sum_{i=1}^{N}(x_{ia} - x_{is})^2}{N}} \tag{8}$$

Table 2. RMSE values calculation for square drawing.

x-axis				*y*-axis			
N	x_{ia}	x_{is}	$(x_{ia} - x_{is})^2$	*N*	y_{ia}	y_{is}	$(y_{ia} - y_{is})^2$
1	0	0	0	1	0	0	0
2	0	0	0	2	0	0	0
.	.	.	.	.	.	.	.
.	.	.	.	.	.	.	.
.	.	.	.	.	.	.	.
400	50	43.59	41.0753	600	50	48.87	1.2611
.	.	.	.	.	.	.	.
.	.	.	.	.	.	.	.
.	.	.	.	.	.	.	.
6270	50	49.93	0.00448	6270	50	49.82	0.03157

From Table 2, a single RMSE drawing can be calculated for the *x* and *y* axes.

$$RMSE_x = \sqrt{\frac{\sum_{i=1}^{N}(x_{ia} - x_{is})^2}{N}} = 0.109279$$

$$RMSE_y = \sqrt{\frac{\sum_{i=1}^{N}(y_{ia} - y_{is})^2}{N}} = 0.060144$$

The RMSE values for square drawing are relatively low, thus the experimental rig showing good accuracy.

6. Conclusions

2-D SMA actuator experimental rig met the aim behind the construction and this can be used for future research for different actuation strategies. SMA spring mathematical calculation has been considered to design and set the shape of the SMA spring. PID combined with tracking mode has been developed to achieve good tracking and good accuracy for the set point.

References

[1] K. Andrianesis, Y. Koveos, G. Nikolakopoulos, and A. Tzes, Experimental study of a shape memory alloy actuation system for a novel prosthetic hand, Shape Memory Alloys, 2010. ISBN: 978-953-307-106-0

[2] L. C. Brinson, “One-dimensional constitutive behavior of shape memory alloys: thermomechanical derivation with non-constant material functions and redefined martensite internal variable”, Journal of intelligent material systems and structures, Vol. 4, Issue 2, pp. 229-242, 1993. https://doi.org/10.1177/1045389X9300400213

[3] C. Liang, and C. A. Rogers, “One-dimensional thermomechanical constitutive relations for shape memory materials”, Journal of intelligent material systems and structures, Vol. 1, Issue 2, pp. 207-234, 1990.

[4] Jong-Ha Chung, Jin-Seok Heo, and Jung-Ju Lee, "Implementation strategy for the dual transformation region in the Brinson SMA constitutive model" Smart Materials and Structures, Vol. 16, No. 1, pp. 1-5, 2006. https://doi.org/10.1088/0964-1726/16/1/N01

[5] P. Nunes, and P. S. Lobo, "Influence of the SMA Constitutive Model on the Response of Structures", Procedia Structural Integrity, Vol. 5, pp. 187-194, 2017. https://doi.org/10.1016/j.prostr.2017.07.098

[6] G. Lange, A. Lachmann, Abdul Hakim Abdul Rahim, M. H. Ismail, and Ch. Y. Low, "Shape memory alloys as linear drives in robot hand actuation", Procedia Computer Science, Vol. 76, pp. 168-173, 2015. https://doi.org/10.1016/j.procs.2015.12.335

[7] P. A. Gédouin, E. Delaleau, J. M. Bourgeot, C. Join, S. Arbab-Chirani, and S. Calloch, "Experimental comparison of classical pid and model-free control: position control of a shape memory alloy active spring", Control Engineering Practice, Vol. 19, No. 5, pp. 433-441, 2011. https://doi.org/10.1016/j.conengprac.2011.01.005

[8] T. A. U. Roshan, B. A. D. J. C. K. Basnayake, Y. W. R. Amarasinghe, D. Wijethunge, and N. D. Nanayakkara, "Development of a PID based closed loop controller for shape memory alloy actuators", 2018 Moratuwa Engineering Research Conference (MERCon), IEEE, pp. 460-464, 2018. https://doi.org/10.1109/MERCon.2018.8421929

[9] C. M. Wayman, and T. W. Duerig, "An introduction to martensite and shape memory" Butterworth-Heinemann, Engineering Aspects of Shape Memory Alloys (UK), pp. 3-20, 1990. https://doi.org/10.1016/B978-0-7506-1009-4.50005-6

[10] S. Nemat-Nasser, and Wei-Guo Guo, "Superelastic and cyclic response of NiTi SMA at various strain rates and temperatures", Mechanics of materials, Vol. 38, Issue 5-6, pp. 463-474, 2006. https://doi.org/10.1016/j.mechmat.2005.07.004

[11] J. Ye, R. K. Mishra, A. R. Pelton, and A. M. Minor, "Direct observation of the NiTi martensitic phase transformation in nanoscale volumes", Acta Materialia, Vol. 58, Issue 2, pp. 490-498, 2010. https://doi.org/10.1016/j.actamat.2009.09.027

[12] I. Mihálcz, "Fundamental characteristics and design method for nickel-titanium shape memory alloy", Periodica Polytechnica Mechanical Engineering, Vol. 45, No. 1, pp.75-86, 2001. https://pp.bme.hu/me/article/view/1410

[13] T. Ishii, "Design of shape memory alloy (SMA) coil springs for actuator applications", Shape Memory and Superelastic Alloys, pp. 63-76, 2011. https://doi.org/10.1533/9780857092625.1.63

[14] Á. V. Peciña, "Design of a shape memory alloy actuator for soft wearable robots", Ph.D. thesis, Electrical Engineering, Electronics and Automation Department, Universidad Carlos III de Madrid, June 2019.